Insight into Polymorphism in Weakly Polar Systems using Favorable Connection Motifs

Yumin Liu[†], Junbo Gong[‖], Dongpeng Yan[*†], Jingkang Wang[‖]

[†] Beijing Key Laboratory of Energy Conversion and Storage Materials, College of Chemistry, and Key Laboratory of Radiopharmaceuticals, Ministry of Education, Beijing Normal University, Beijing 100875, China;

[‖] School of Chemical Engineering and Technology, Collaborative Innovation Center of Chemical Science and Chemical Engineering, Tianjin University, Tianjin 300072, P. R. China

E-mail: yandp@bnu.edu.cn

S1 Experimental methods

S1.1 Materials

Dibenzoylmethane (DBM, 99.0%), methanol (≥99.5%), ethanol (≥99.5%), 2-propanol (IPA, ≥99.5%), ethyl acetate (≥99.5%), acetonitrile (≥99.5%) and toluene (≥99.5%) were purchased from Shanghai Titan Science & Technology Co. Ltd. and used as-received without any further purification.

S1.2 Solubility measurements

The solubility of dibenzoylmethane form I in six different polar solvents was measured at various temperatures using a gravimetric method. Saturated solutions with excess form I DBM in double-jacketed glass vessels were continuously stirred by an electric magnetic stirrer for roughly 24 h to ensure the solid-liquid equilibrium. The temperature of solutions was kept by a thermostatic bath (Julobo CF41, Germany) with an uncertainty of ± 0.01 °C. About 5 mL of the upper clear saturated solution was taken out after the suspension settled for 2 h by using a disposable syringe and filtered (0.22 μm PTFE filter) into a pre-weighed vial. The vials were then put in the fume hood for solvent evaporation until the total weight did not change at room temperature. Each experiment was repeated at least five times and the mean values

were used as the final solubility data. An analytical balance (ME204T/02, Metler Toledo, Shanghai Company) with a precision of ± 0.0001 g was used during the whole experimental processes. Powder X-ray diffraction (PXRD, Rigaku D/max 2500 X, scanned between 2° and 40° at 8 °/min and a step size of 0.02°) was used to make sure that the forms are the same in solubility measurement. Fig. S1.2 shows that there no phase transformation happened during the solubility measurement processes.

Table S1 Solubility data of DBM form I in g DBM/kg Solvent

T (°C)	methanol	ethanol	isopropanol	ethyl acetate	acetonitrile	toluene
0	16.78	22.21	10.69	262.66	76.98	205.83
5	21.09	26.82	13.16	317.05	97.87	255.22
10	24.90	32.01	17.19	377.24	130.05	317.35
15	28.96	38.62	20.78	446.44	169.76	389.71
20	38.70	46.36	29.62	556.79	239.32	491.14

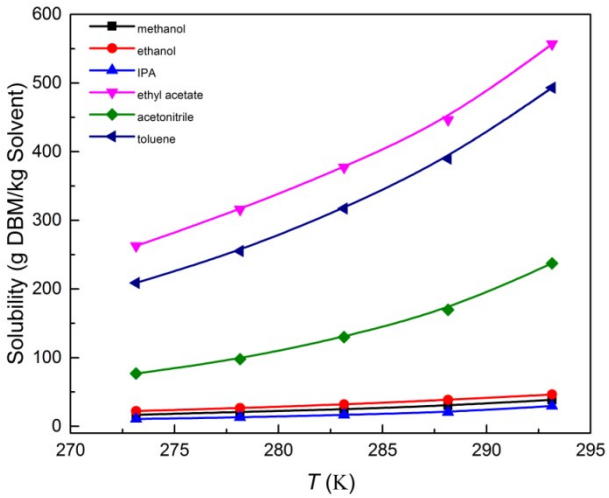

Fig. S1.1 Solubility data of DBM

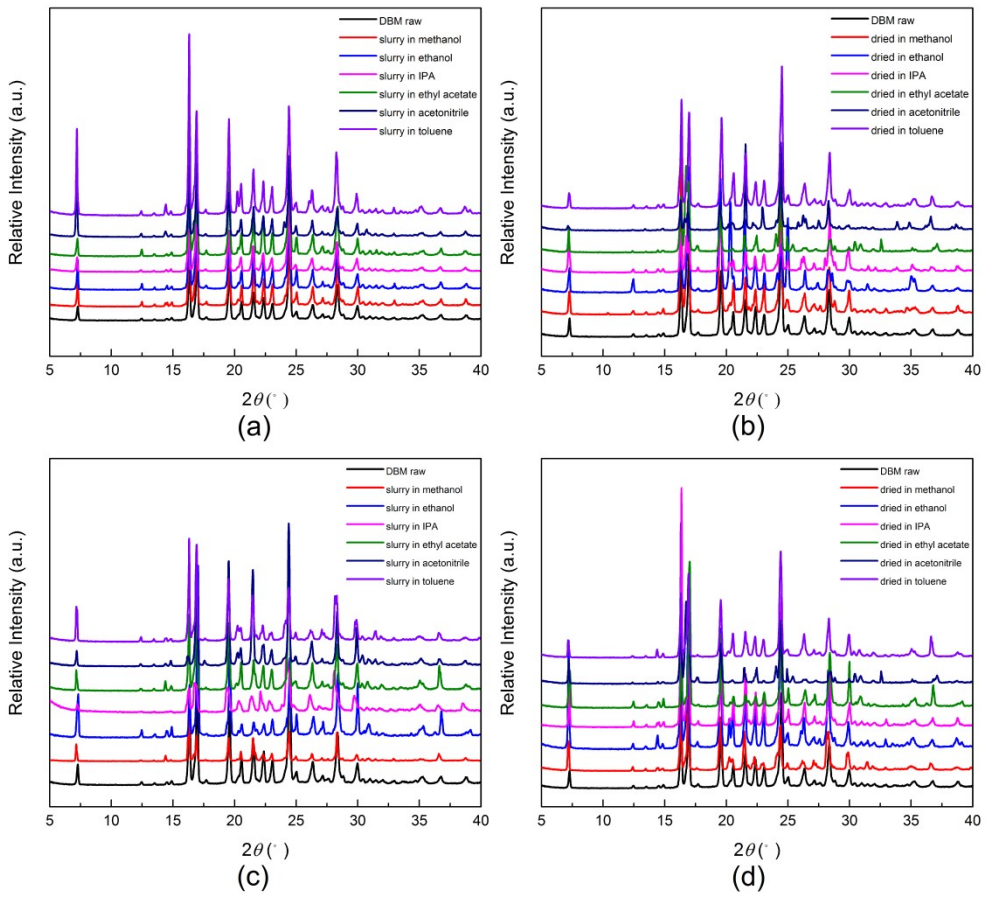

Fig. S1.2 PXRD patterns of the slurry phases and dried products of DBM in various solvents at two different temperatures of 0 °C and 20 °C: (a) slurry at 0 °C; (b) dried products at 0 °C; (c) slurry at 20 °C; (d) dried products at 20 °C

S1.3 Batch crystallisation experiments

S1.3.1 Slow evaporation

Single crystals of DBM polymorphs were grown by slow evaporation in six different polar solvents at room temperature. Saturated solutions at 20 °C were made by completely dissolving desired commercial powder into methanol, ethanol, isopropanol, ethyl acetate, acetonitrile and toluene. Clear solutions were filtered with the 0.22 μm filters (PTFE membranes) into glass vials sealed by parafilms with several holes in the centre only. All vials were left in the fume hood for several days allowing crystals to crystallize after the evaporation of solvents. Powder X-ray diffraction (PXRD, Rigaku D/max 2500 X, scanned between 2° and 40° at 8 °/min and a step size of 0.02°, samples were ground with a pestle and mortar for PXRD analysis), single crystal x-ray diffraction (SCXRD, Rigaku-Oxford FR-X DW, MoKα,

λ=0.71073 Å), fourier transform infrared spectrometer (ATR-FTIR, Bruker, scanned between 4000 cm^{-1} and 400 cm^{-1} with resolution of 4 cm^{-1}) and Raman microscope (Thermo Scientific DXR, scanned between 3500 cm^{-1} and 50 cm^{-1}) were used for polymorph identification and comparison. Differential scanning calorimetry (Mettler Toledo DSC 1/500, 20 K/min, 5-10 mg, N_2 protection) was used to study thermal behaviour of DBM polymorphs. Optical microscopy (Zeiss Axioplan 2) was used to compare crystal morphologies of DBM polymorphs. We observed that block form I and needle-like form III were concomitantly grown in toluene by slow evaporation at room temperature. The ATR-FTIR and Raman spectra suggests that a high similarity exists between the weak intermolecular interactions for forms I and III.

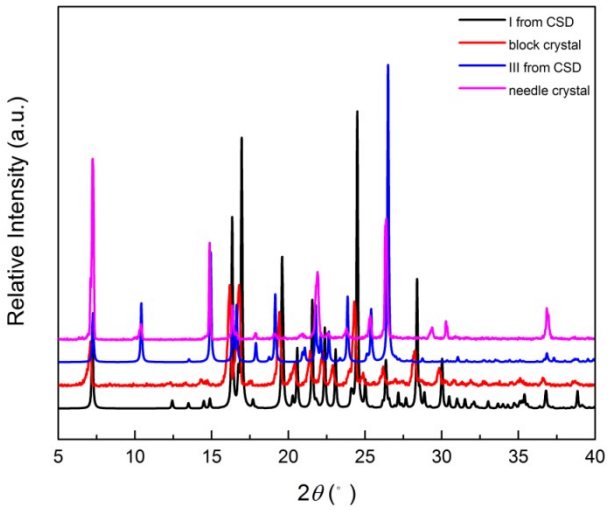

Fig. S1.3 Powder x-ray powder diffraction patterns of DBM products during slow evaporation experiments in toluene at room temperature

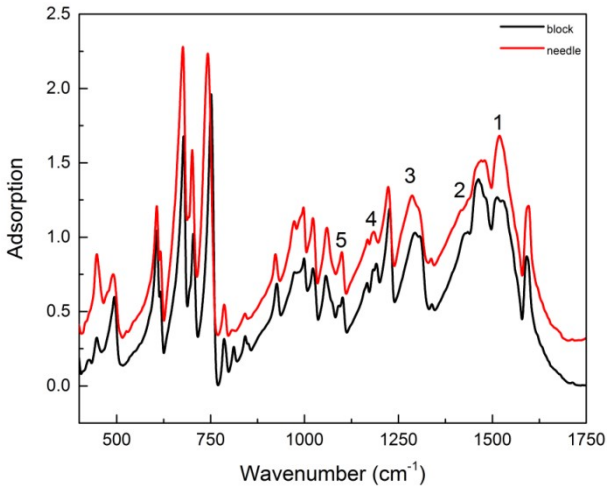

Fig. S1.4 ATR-FTIR patterns of DBM products during slow evaporation experiments in toluene at room temperature

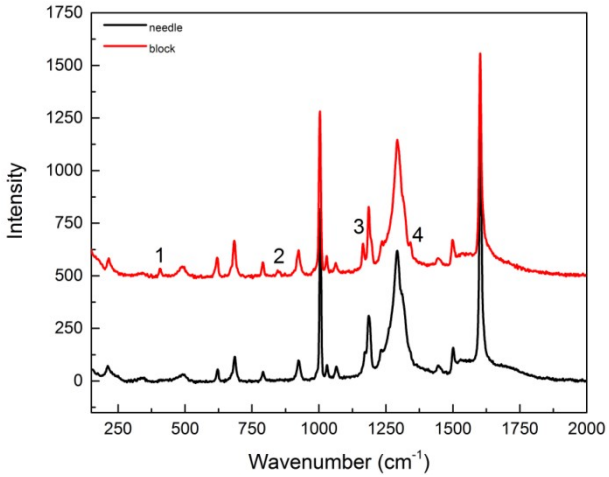

Fig. S1.5 Raman patterns of DBM products during slow evaporation experiments in toluene at room temperature

S1.3.2 Crash cooling crystallisation

Simple batch crystallizations with various supersaturations were carried out in order to crystallize powder of DBM form III. 20 g of solvents (methanol, ethanol, isopropanol, ethyl acetate, acetonitrile and toluene) along with the appropriate amount (depending on the required supersaturation) commercial DBM was prepared in 50 mL jacketed vessels with magnetic stirring. The solution temperature was heated to ~10-15 °C above the chosen crystallization temperature to make the powder dissolve completely. The vessel was then rapidly cooled to the crystallization temperature (0 °C or 20 °C) to allow crystals to crystallise. The solution was filtered as soon as crystals appeared to avoid transformation to form I. It is apparent that in Table S2

only the block form I DBM crystallized in crash cooling conditions. In one sense, the needle-like form III DBM exhibits “difficult to crystallise”.

Table S2 Polymorphic crystallization results for DBM under different supersaturations and various temperatures during batch experiments

	methanol	ethanol	isopropanol	ethyl acetate	acetonitrile	toluene
SE	I/III	I/III	I/III	I/III	I/III	I/III
CC	I	I	I	I	I	I

SE and CC respectively mean slow evaporation and crash cooling.

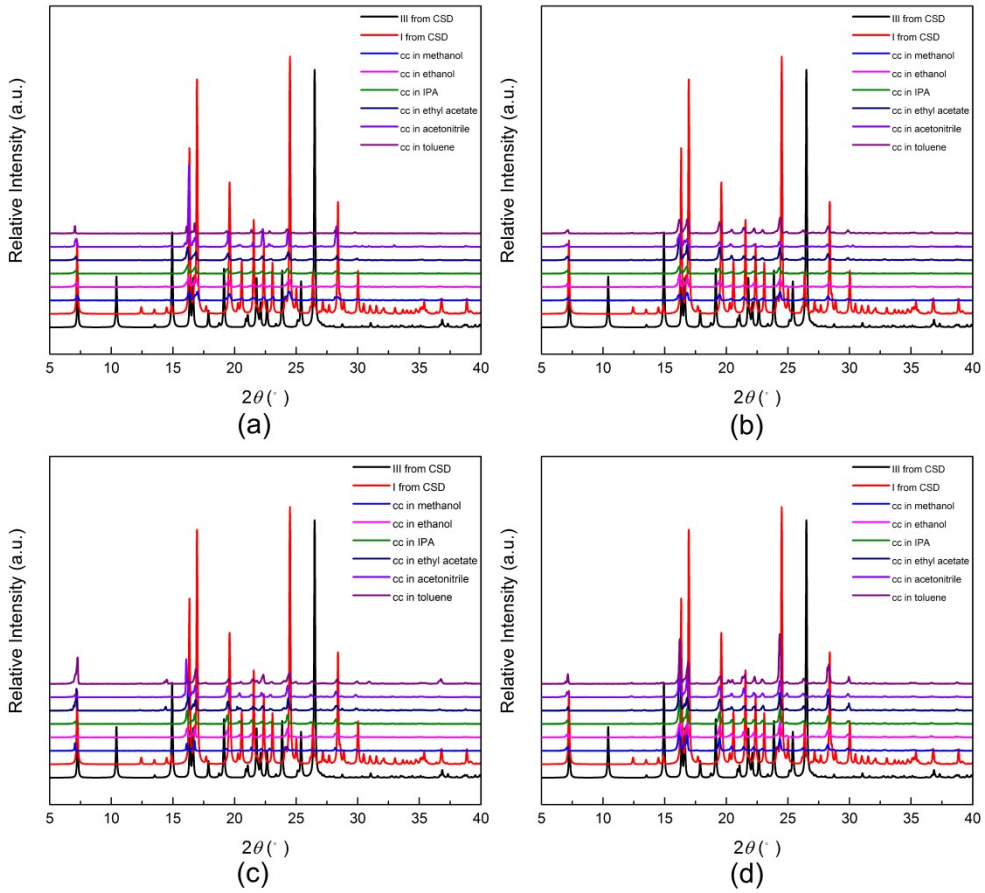

Fig. S1.6 Powder x-ray diffraction patterns of DBM products during nucleation experiments in various solvents at two different temperatures of 0 °C and 20 °C: (a) 0 °C, $S = 2.5$; (b) 0 °C $S = 4.0$; (c) 20 °C, $S = 2.5$; (c) 20 °C, $S = 4.0$

S1.3.3 Solvent-mediated phase transformation experiments

Solvent mediated phase transformation experiments (also known as slurries) in

methanol at 20 °C were carried out by *in situ* monitoring crystal growth of DBM form III. A seed crystal of DBM form III was put into a supersaturated solution with the supersaturation of 1.25 and the phase transformation process was observed by using an inverted microscope (Olympus CKX41). Each experiment was based on a new crystal seed and was repeated at least three times to check the repeatability and accuracy. Experiments resulted in the transformation of DBM form III to the more stable form I.

S2 Crystal form comparisons

S2.1 Overall weak intermolecular interactions

The overall weak hydrogen bonds observed in all three forms of DBM are shown in Fig. S2.1. It is evident that the three structures have significant similar weak H-bonding.

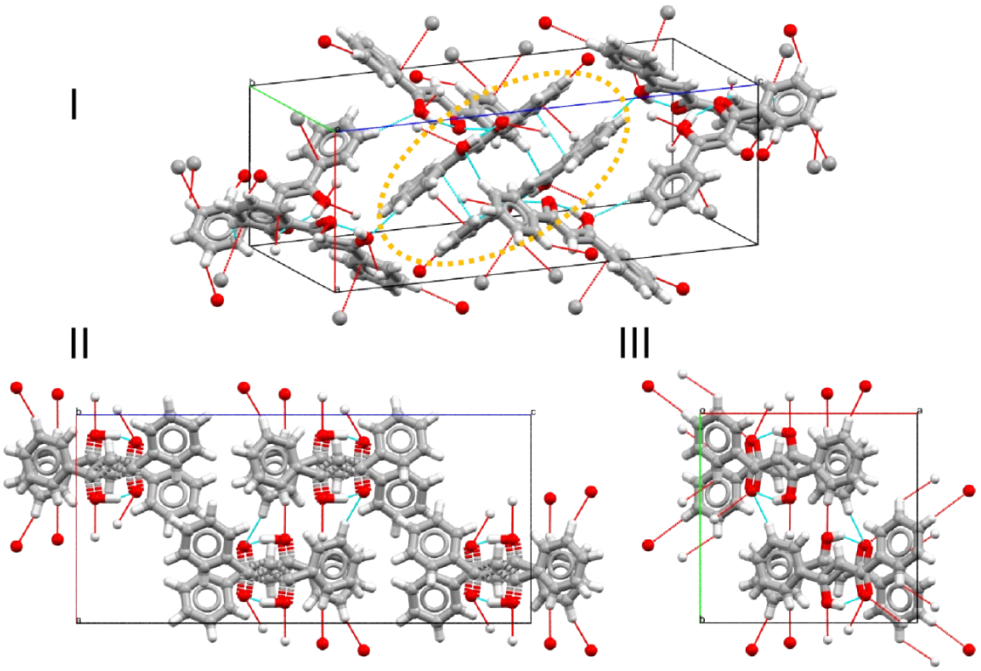

Fig. S2.1 Unit cell view of the three DBM polymorphs

S2.2 Crystal packing similarity

The crystal structure of DBM forms I to III was compared by using the CSD Materials crystal packing similarity tool. The results of the comparison, namely the number of overlapping molecules (out of 30) with the associated rmsd are reported in Table S2.1 below. It is concluded that the crystal packing of three DBM polymorphs has little similarity although their overall weak intermolecular interactions are very

similar.

Table S3 Numerical values of comparisons between crystal structures of DBM polymorphs

Form[a,b]	CSS[c]	rmsd [Å]
I/II	1	0.265
I/III	1	0.1333
II/III	10	3.468

[a]Crystal structures obtained in experiments were used for forms I and III, respectively

[b]DBEZLM03 retrieved from the Cambridge Structural Database (CSD) was used for form II.

[c]Crystal Structure Similarity (out of 30 molecules)

S3 Analyses of torsion angles in DBM form I

The mean plane and torsion angle of DBM molecule in form I are shown in Fig. S3.1. It is noted that in DBM forms I the two phenyl rings are almost coplanar.

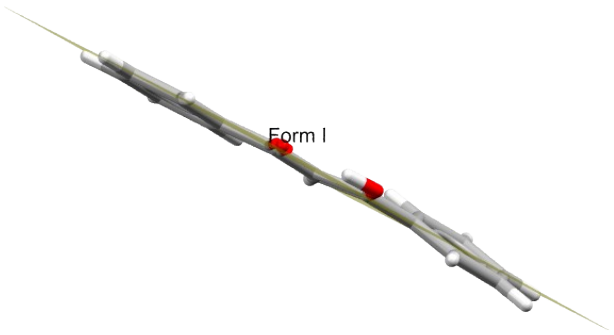

Fig. S3.1 The mean plane of DBM molecule in form I

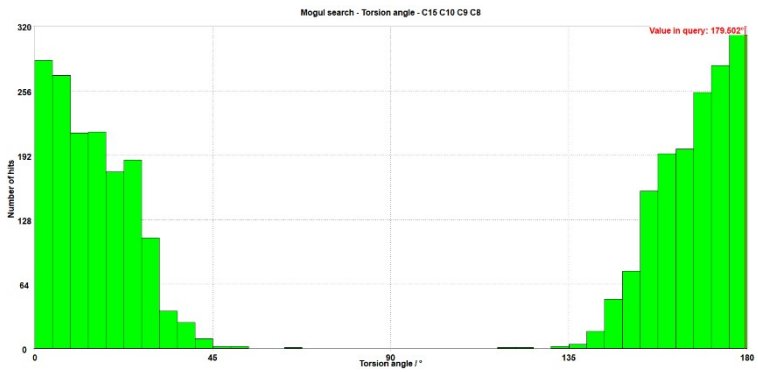

Fig. S3.2 The torsion angle of DBM molecule in form I

S4 Justification for cut-off at 4.70 Å

The C···C, C···H and H···H energies as a function of the interatomic distances in DBM form II and III were shown in Fig. S3.1 and Fig. S3.2. It is clear that in DBM forms II and III C…C connections out to 4.7 Å are also more attractive than all C…H and H…H connections.

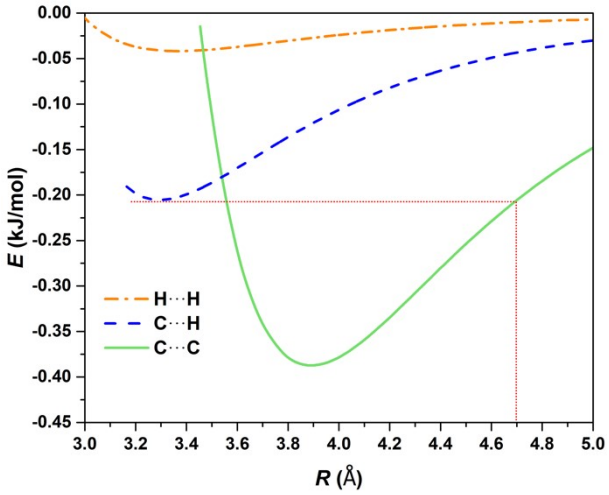

Fig. S4.1 The C···C, C···H and H···H energies as a function of the interatomic distances in DBM form II

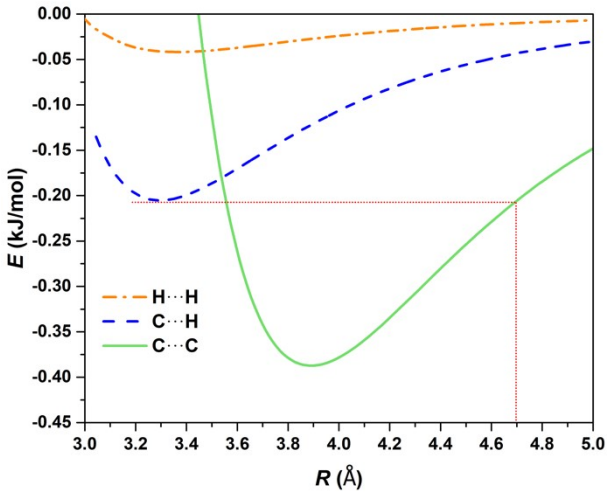

Fig. S4.2 The C···C, C···H and H···H energies as a function of the interatomic distances in DBM form III

S5 Comparison of N_{FC} and UNI interaction energies

UNI was selected to study the relationship between N_{FC} and interaction energies in DBM polymorphs which is shown in Fig. S5.1. The specific calculation steps are as follows: Click on the *CSD-Materials* and then *Calculations* in the top-level menu. In the *Calculations* dialogue box, choose *UNI intermolecular potentials* from the

resulting drop-down menu. This will open the *intermolecular potentials* dialogue box. We kept the default settings. The strongest aromatic stacking interactions in the crystal structure of DBM polymorphs would be generated in the *Output* section. It is noted that the geometric N_{FC} method ranks the interactions in the same order as the UNI calculations (the comparison uses the absolute value of interaction energies).

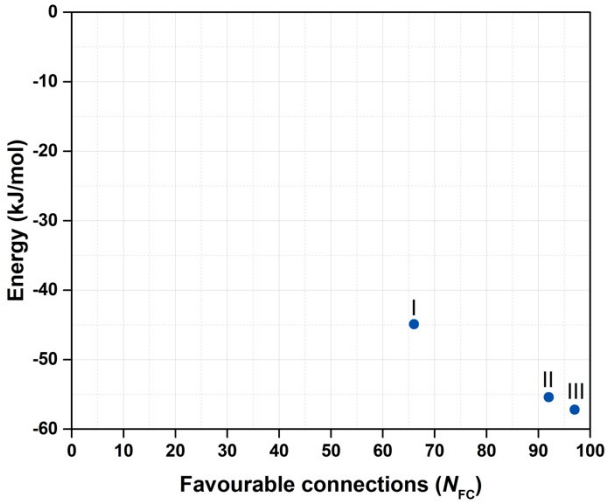

Fig. S5.1 The relationship between N_{FC} and interaction energies of DBM dimer molecules

S6 Aromatic analyser results for DBM polymorphs

S6.1 Face···face distances between the strongest interacting dimer molecules

The analysis of the face···face interplanar separations in all DBM polymorphs is shown in Fig. S6.1 to Fig. S6.3, which suggests that a compromise between torsion angles optimizing and utilisation of strongest possible face···face approach results in the polymorphism of DBM molecule.

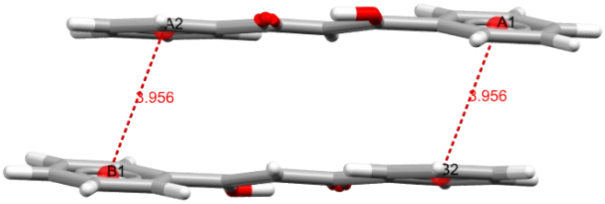

Fig. S6.1 Face···face distances between the strongest interacting dimer molecules in DBM form I

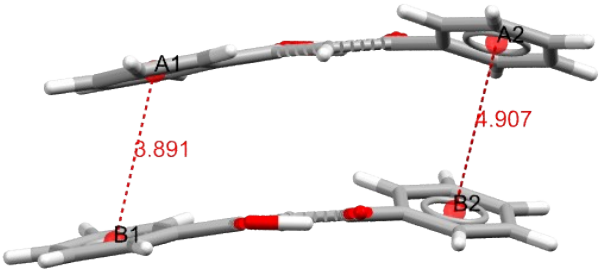

Fig. S6.2 Face···face distances between the strongest interacting dimer molecules in DBM form II

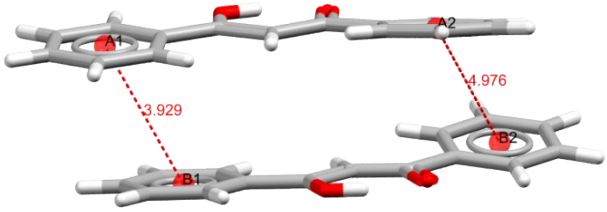

Fig. S6.3 Face···face distances between the strongest interacting dimer molecules in DBM form III

S6.2 Weaker intermolecular interactions in DBM polymorphs

The strongest DBM···DBM interactions between cetroid1,2_ cetroid19,20 molecules in DBM form I, cetroid1,2_ cetroid25,26 molecules in DBM form II and cetroid1,2_ cetroid25,26 molecules in DBM form III are described in the main text.

S6.2.1 DBM form I

The aromatic analyser identifies five strong phenyl…phenyl approaches in DBM form I.

	Centroid1	Centroid2	Distance	Relative Orientatior	Inter-lecul	Score	Assessment
1	1	20	3.96	13.06	Yes	9.6	Strong
2	2	19	3.96	13.06	Yes	9.6	Strong
3	2	22	4.29	0	Yes	9.1	Strong
4	1	23	4.96	67.61	Yes	7.8	Strong
5	1	25	4.96	67.61	Yes	7.8	Strong
6	1	7	5.98	34.27	Yes	5.7	Moderate
7	1	9	5.98	34.27	Yes	5.7	Moderate

Fig. S6.4 Strong approaches from the aromatic analyser output for DBM form I

The weaker DBM···DBM interactions between cetroid1,2_cetroid21,22 molecules, cetroid1,2_cetroid23,24 molecules and cetroid1,2_cetroid25,26 molecules in DBM form I are shown in Table S6.1, Fig. S6.5, Fig. S6.6 and Fig. S6.7.

Table S4 Weaker favourable connections in DBM form I

	cetroid1,2_cetroid21,22[a]		cetroid1,2_cetroid23,24[b]		cetroid1,2_cetroid25,26[b]	
FC	N_{FC}	Colour/type	N_{FC}	Colour/type	N_{FC}	Colour/type
OH···A1			5	orange	5	orange
OH··A2	6	orange				
OH··B2	6	orange				
C=O··A2	12	blue				
C=O···B2	12	blue				
=CH-···A2	4	purple				
=CH-···B2	4	purple				
A1···B1			10	green	10	green
A2···B2	22	green				
Total	66	Inversion	Glide		Glide	

[a,b]face-to-face and face-to-edge

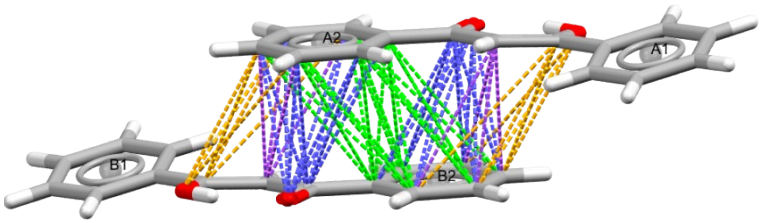

Fig. S6.5 Weaker intermolecular interactions between cetroid1,2_cetroid21,22 molecules in DBM form I

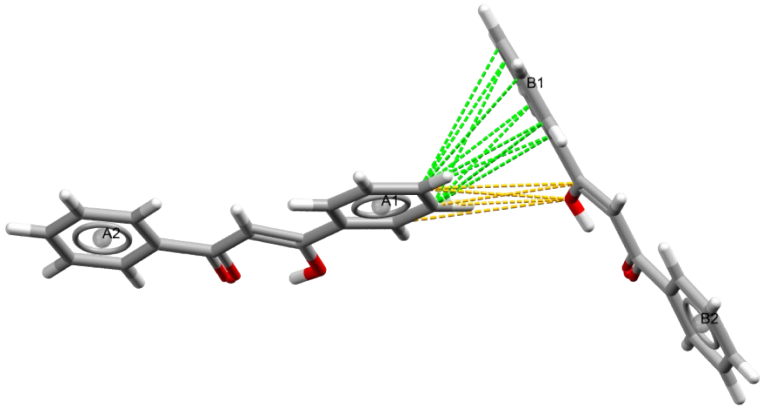

Fig. S6.6 Weaker intermolecular interactions between cetroid1,2_cetroid23,24 molecules in DBM form I

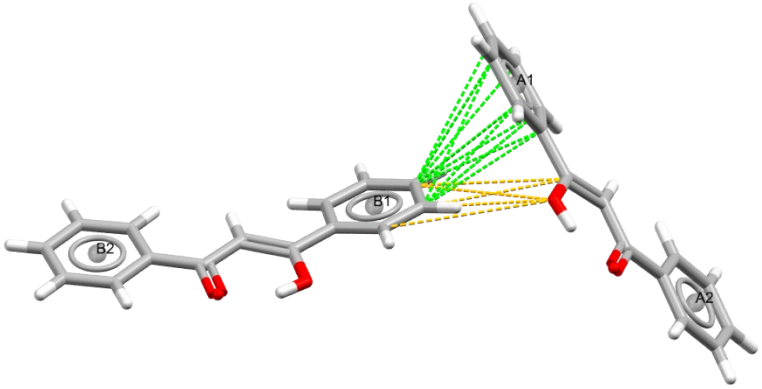

Fig. S6.7 Weaker intermolecular interactions between cetroid1,2_cetroid25,26 molecules in DBM form I

S6.2.2 DBM form II

The aromatic analyser identifies four strong phenyl…phenyl approaches in DBM form II

	Centroid1	Centroid2	Distance	Relative Orientation	Inter-lecul	Score	Assessment
1	1	23	3.89	9.01	Yes	9.5	Strong
2	1	25	3.89	9.01	Yes	9.5	Strong
3	2	24	4.91	34.69	Yes	7.2	Strong
4	2	26	4.91	34.69	Yes	7.2	Strong
5	2	12	5.11	34.86	Yes	6.6	Moderate
6	2	14	5.11	34.86	Yes	6.6	Moderate

Fig. S6.8 Strong approaches from the aromatic analyser output for DBM form II

The weaker DBM···DBM interactions between cetroid1,2_cetroid25,26 molecules

in DBM form II are shown in Table S6.2 and Fig. S6.9.

Table S5 Weaker favourable connections in DBM form II

	cetroid1,2_ cetroid25,26	
FC	N_{FC}	Colour/type
OH···OH	3	cyan
OH···=CH-	4	violet
OH···C=O	3	cyan
OH···A1	1	orange
OH··A2	4	orange
OH··B1	11	orange
C=O···C=O	3	cyan
C=O···=CH-	4	violet
C=O··A2	9	blue
C=O···B1	1	blue
C=O···B2	5	blue
=CH-···=CH-	1	light green
=CH-···A2	2	purple
=CH-···B1	3	purple
A1···B1	27	green/face-to-face
A2···B2	11	Green/ tilted
Total	92	Glide

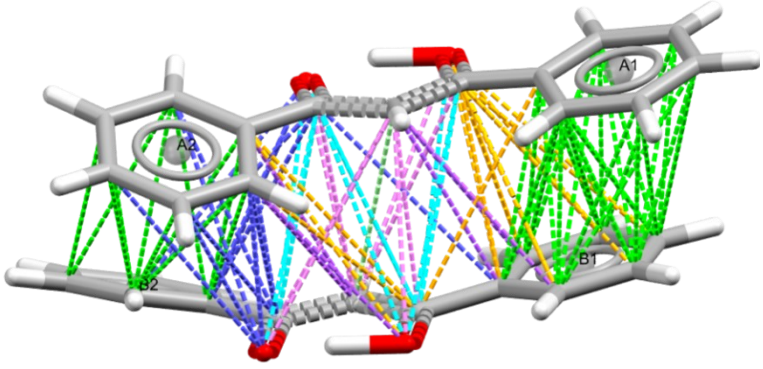

Fig. S6.9 Weaker intermolecular interactions between cetroid1,2_cetroid25,26 molecules in DBM form II

S6.2.3 DBM form III

The aromatic analyser identifies five strong phenyl…phenyl approaches in DBM form III

	Centroid1	Centroid2	Distance	Relative Orientation	Inter-lecul	Score	Assessment
1	1	25	3.93	7.37	Yes	9.6	Strong
2	1	27	3.93	7.37	Yes	9.6	Strong
3	2	26	4.98	19.33	Yes	7.7	Strong
4	2	28	4.98	19.33	Yes	7.7	Strong
5	2	20	5.31	0	Yes	7.4	Strong
6	1	4	5.61	13.65	Yes	6.9	Moderate
7	2	5	5.61	13.65	Yes	6.9	Moderate

Fig. S6.10 Strong approaches from the aromatic analyser output for DBM form III

The weaker DBM···DBM interactions between cetroid1,2_cetroid27,28 molecules and cetroid1,2_cetroid19,20 in DBM form III are shown in Table S6.3, Fig. S6.11 and Fig. S6.12.

Table S6 Weaker favourable connections in DBM form III

	cetroid1,2_ cetroid27,28		cetroid1,2_ cetroid19,20	
FC	N_{FC}	Colour/type	N_{FC}	Colour/type
OH···OH	3	cyan		
OH···=CH-	4	violet		
OH···C=O	3	cyan		
OH···A1	11	orange		
OH··B2	6	orange		
C=O···C=O	3	cyan		
C=O···=CH-	3	violet		
C=O··A1	4	blue		
C=O··A2	3	blue		
C=O···B2	11	blue		
=CH-···=CH-	1	light green		

=CH-···A1	4	purple		
=CH-···B2	3	purple		
A1···B1	26	green		
A2···B2	12	green	7	green
Total	97	Glide/face-to-face	7	Glide/face-to-face

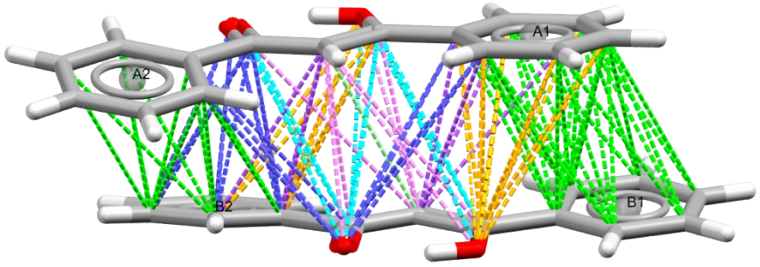

Fig. S6.11 Weaker intermolecular interactions between cetroid1,2_cetroid27,28 molecules in DBM form III

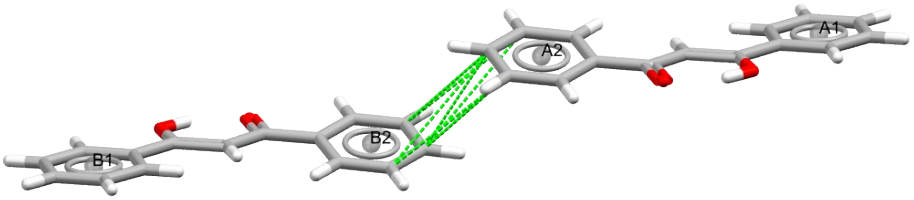

Fig. S6.12 Weaker intermolecular interactions between cetroid1,2_cetroid19,20 molecules in DBM form III